TRACKING VIRUS PARTICLES IN FLUORESCENCE MICROSCOPY IMAGES USING TWO-STEP MULTI-FRAME ASSOCIATION

A. Jaiswal[1], W. J. Godinez[1], R. Eils[1], M. J. Lehmann[2], K. Rohr[1]

[1]University of Heidelberg, BIOQUANT, IPMB, and DKFZ Heidelberg,
Dept. Bioinformatics and Functional Genomics, Biomedical Computer Vision Group,
Im Neuenheimer Feld 267, 69120 Heidelberg, Germany
[2]Humboldt-University Berlin, Molecular Parasitology, Philippstrasse 13, 10115 Berlin, Germany

ABSTRACT

Automatic fluorescent particle tracking is an essential task to study the dynamics of a large number of biological structures at a sub-cellular level. We have developed a two-step multi-frame association finding algorithm which is based on a temporally semi-global formulation as well as combines a spatially global and a spatially local approach. Using this multi-frame association finding algorithm we have developed a probabilistic tracking approach based on the Kalman filter. We have successfully applied the approach to synthetic as well as real microscopy image sequences of ALV virus particles and quantified the performance. We found that the proposed approach outperforms previous approaches.

Index Terms— Virus particle tracking, multi-frame association, Kalman filter.

1. INTRODUCTION

Automatic tracking of subcellular structures in fluorescence microscopy images is important to study the behavior of, for example, virus particles under different experimental conditions. Virus particle tracking is challenging due to the similar appearance of different virus particles, the high particle density, the large number of spurious objects, the appearance and disappearance of particles, as well as their hardly predictable motion. Moreover, a high level of noise, frequent clustering and unclustering of the virus particles, and out-of-focus movement of the virus particles are additional challenges for an automatic tracking algorithm.

Previous work on *particle tracking* can be subdivided into deterministic and probabilistic approaches. *Deterministic* approaches consist of particle detection and association finding (e.g., [1, 2]). While being computationally efficient, deterministic approaches often have difficulties in dealing with spurious objects and detection errors [3]. In contrast, *probabilistic* approaches perform spatial-temporal filtering to robustly estimate the position of particles under noisy conditions [3, 4]. Thus, probabilistic approaches generally outperform deterministic approaches. However, a disadvantage of probabilistic approaches is that for multiple particle tracking typically a deterministic association finding approach is employed which takes into account only two frames.

Approaches for *association finding* can be characterized on the basis of their *temporal* and *spatial* scope. Regarding the *temporal scope*, approaches for association finding can be categorized as *two-frame* (e.g., [3, 4]) or *multi-frame* (e.g., [2, 5, 6, 7]) approaches. *Two-frame* approaches do not cope well with difficult tracking tasks (e.g., appearance and disappearance of particles) for which information from multiple frames is important. In contrast, *multi-frame* approaches (e.g., [5]) exploit more temporal information. However, the computational cost increases exponentially with the number of time points. The efficient deterministic approach in [1] achieves multi-frame association by multiple two-frame associations. Thus, the approach is in fact temporally local (*two-frame* approach). Deterministic association finding approaches that uncouple particle linking from the detection of clustering and unclustering events (e.g., [6]) are prone to yield incorrect associations because they do not fully exploit the available information. Deterministic [2] and probabilistic [7] multi-frame association finding algorithms perform particle linking and detection of clustering and unclustering simultaneously. However, these approaches are *spatially global* and consider all particles simultaneously at a time point. This may lead to incorrect associations in the presence of a large number of spurious objects because locally highly likely associations may not be included in the global optimal solution.

In this work, we have developed a two-step multi-frame association finding algorithm which is based on a temporally semi-global formulation as well as combines a spatially global and a spatially local approach. Using this multi-frame association finding algorithm we have developed a probabilistic tracking approach based on the Kalman filter. Compared to spatially global approaches, our association finding algorithm can better cope with spurious objects by selecting highly likely associations in the first step and using multi-frame optimization for the unmatched particles in the second step. Key properties of our approach are multi-frame

optimization, verification of associations with past and subsequent positions of the particles, correction of erroneous associations, and robust estimation of the position of particles. Compared to [1], our approach simultaneously exploits the information from several consecutive time points. Unlike [6], our approach performs particle linking and detection of clustering and unclustering simultaneously. We have quantitatively evaluated our approach using synthetic as well as real fluorescence microscopy image sequences displaying avian leukosis virus (ALV) particles and performed a comparison with previous approaches.

2. MULTI-FRAME BASED PARTICLE TRACKING

2.1. Two-step association (TSA)

We model the association finding problem using a w-partite graph for a temporal window of size w. Vertices of the graph represent particles and edges of the graph denote possible associations. The edges are assigned weights that correspond to the likelihood of the association. Partite sets of the graph correspond to the set of measured (or predicted) positions of the particles at time points within the window. For a particle i at time point t, with position $\boldsymbol{p}_t^i$ and a particle j, at time point $t+r$, with position $\boldsymbol{p}_{t+r}^j$, where $r \epsilon [1, 2, ..., w-1]$, the likelihood that the two particles correspond to the same object over time is given by the following gain function:

$$g(\boldsymbol{p}_t^i, \boldsymbol{p}_{t+r}^j) \quad = \quad 1 - \frac{\|\boldsymbol{u} - \boldsymbol{v}\|_2}{\sqrt{s_x^2 + s_y^2}} \tag{1}$$

where $\boldsymbol{u} = \hat{\boldsymbol{p}}_{t+r}^i - \boldsymbol{p}_t^i$ and $\boldsymbol{v} = \boldsymbol{p}_{t+r}^j - \boldsymbol{p}_t^i$ are the predicted and measured displacement vectors, respectively, and $\hat{\boldsymbol{p}}_{t+r}^i$ is the predicted position at time point $t+r$. Here, s_x and s_y are the image dimensions.

We have developed a two-step multi-frame association algorithm (TSA) which combines a spatially local and a spatially global approach. First, reliable associations are generated in a spatially and temporally local manner. This step is called reliable association generation (RAG). Second, for the particles that remain unassociated in the first step, a multi-frame association (MFA) algorithm is used which performs spatially global and temporally semi-global optimization. For each particle, the search for associations is performed in predefined neighborhoods. For the two steps, we use two different circular neighborhoods represented by two circles with different radii r_1, r_2 centered at a particle. The first neighborhood Ω_1 corresponds to the region of the smaller circle and the second neighborhood Ω_2 corresponds to the region between the two circles .

By using pairs of consecutive frames, RAG generates highly likely associations on the basis of an application dependent criterion (e.g., displacement, intensity). We use RAG for establishing associations corresponding to particles exhibiting confined motion. Therefore, we set the radius r_1 of Ω_1 equal to the average size of the particles and generate all feasible associations. We use a local nearest neighbor approach to find an association for which the gain is maximal:

$$\arg\max_j (g(\boldsymbol{p}_{t+r-1}^i, \boldsymbol{p}_{t+r}^j)) \tag{2}$$

The MFA uses Ω_2 to generate associations. We define the radius r_2 of Ω_2 on the basis of the maximum possible displacement of the particles. This discards very unlikely associations. The MFA establishes associations for all unassociated particles within the temporal window. The MFA initially generates soft associations which can be changed when more information becomes available. The soft associations between the first two frames within a temporal window are changed into hard associations only after processing all frames within the window. A split graph has been constructed from a w-partite graph for a temporal window of size w [2]. The optimal solution corresponds to the maximum matching of the split graph. The optimization objective has been defined as finding a hypothesis $\boldsymbol{M}_{max}$ with the maximum total gain from the set of all hypotheses C:

$$\boldsymbol{M}_{max} = \arg\max_{\boldsymbol{M} \epsilon \boldsymbol{C}} \sum_{(\boldsymbol{p}_t^i, \boldsymbol{p}_{t+r}^j) \epsilon \boldsymbol{M}} g(\boldsymbol{p}_t^i, \boldsymbol{p}_{t+r}^j) \tag{3}$$

$$\text{subject to: } \sum_{k=1}^{N} \boldsymbol{M}_{k,l} = 1, \sum_{l=1}^{N} \boldsymbol{M}_{k,l} = 1,$$

where N is the total number of measurements and predictions within a temporal window. A hypothesis $\boldsymbol{M}$ is a feasible solution represented by an association matrix consisting of 0 and 1, where 1 indicates presence of the association and 0 indicates absence of the association in the solution. The constraints ensure a one-to-one association. We solve the optimization problem (3) using the Hungarian algorithm. The two steps of TSA (RAG & MFA) are performed alternatingly. RAG iteratively generates reliable associations for all frames within a window. MFA progressively processes all frames as the window is initialized by two frames and with every iteration the window is enlarged by one frame until it reaches its full size (i.e. w frames). RAG always processes the last two frames within the temporal window and MFA exploits all frames within the growing temporal window.

2.2. Probabilistic tracking approach using multiple frames

We have developed a probabilistic tracking approach that combines the deterministic two-step multi-frame association (TSA) algorithm described above with the Kalman filter (KF), and is denoted by TSAKF. A block diagram of TSAKF is shown in Figure 1. A set of predicted positions of the particles at a time point t is denoted by $\hat{\boldsymbol{P}}_t$ and a set of measured positions of the particles at time point t is denoted by $\boldsymbol{P}_t$. TSA uses as input $\hat{\boldsymbol{P}}_t$ and the measured positions of the particles at time points $t, t+$

$1, ..., t + w - 2$, namely $\boldsymbol{P}_t, \boldsymbol{P}_{t+1}, ..., \boldsymbol{P}_{t+w-2}$ for a temporal window of size w. Thus, the input for TSA consists of $\hat{\boldsymbol{P}}_t, \boldsymbol{P}_t, \boldsymbol{P}_{t+1}, ..., \boldsymbol{P}_{t+w-2}$. The goal of TSA is to find associations between $\hat{\boldsymbol{P}}_t$ and $\boldsymbol{P}_t$ by exploiting the information in all frames within the window. Based on the association results of TSA, the KF determines an estimate of the positions of the particles at the current time point.

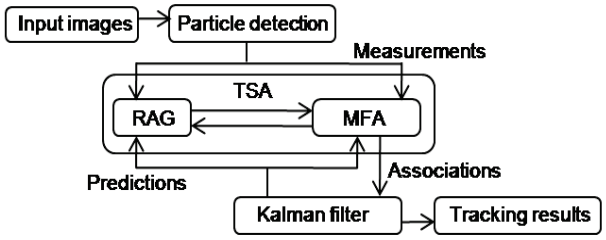


Fig. 1. Diagram of TSAKF tracking approach

3. EXPERIMENTAL RESULTS

We have applied the developed approach (TSAKF) to synthetic data and real microscopy image sequences of avian leukosis virus (ALV) particles. We have also applied two other approaches: the deterministic approach TSA, and a probabilistic approach that combines MFA with KF (MFAKF). For a comparison, we also applied three previous approaches: a two-frame deterministic approach (TFA) [1], a deterministic approach based on multi-frame association (MFA) [2], and a KF based tracking approach which uses TFA for motion correspondence [4]. In total, we have evaluated six tracking approaches.

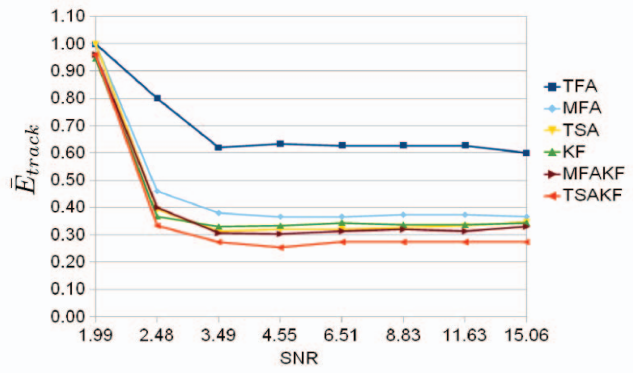


Fig. 2. Tracking results for synthetic image sequences as a function of the SNR level (mean track error $\bar{E}_{track}$)

The synthetic images have been generated to simulate real fluorescence microscopy images. An advantage is that ground truth is available. The synthetic image sequences show multiple particles with different motion patterns and a high object density. To evaluate the approaches under different conditions, we generated synthetic image sequences for 8 different levels of the signal-to-noise ratio (SNR) and 10 different

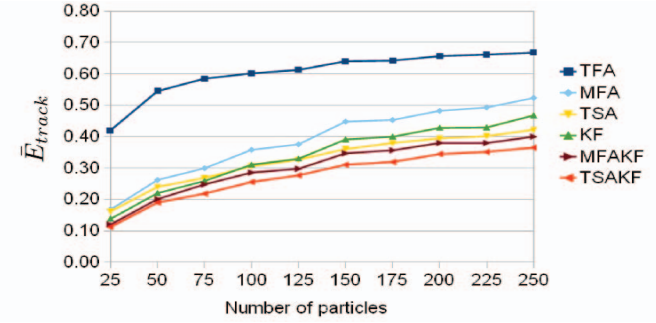


Fig. 3. Tracking results for synthetic image sequences as a function of the number of particles (mean track error $\bar{E}_{track}$)

levels of object density (number of particles). The SNR is calculated as the ratio of the difference between the peak intensity of a particle I_{max} and the intensity of the background I_b, and the noise level σ_n. To quantitatively evaluate the performance of the tracking approaches we computed the track error E_{track}, which is defined based on the number of the correct trajectories $n_{track,correct}$ and the total number of the true trajectories $n_{track,total}$ as: $E_{track} = 1 - \frac{n_{track,correct}}{n_{track,total}}$. A trajectory is considered to be correct if it contains more than 75% correct positions (positions within a tolerance of 2 pixels). Fixed parameter values have been used for all image sequences. For particle detection, we have used the spot enhancing filter [8]. Since the virus particles exhibit random motion, we set the predicted position of a particle to its previous position. The radii of Ω_1 and Ω_2 have been set to $r_1 = 3$ pixels and $r_2 = 10$ pixels, respectively, in accordance with the image data. We have used a temporal window of size $w = 5$. We generated 20 synthetic image sequences for each of the 8 different SNR levels (1.99, 2.48, 3.49, 4.55, 6.51, 8.83, 11.63, 15.06) and for each of the 10 different levels of object density (25, 50, 75, 100, 125, 150, 175, 200, 225, 250), and computed the mean track error $\bar{E}_{track}$ (see Figures 2 and 3). In total, we used 360 image sequences each with 100 frames. Regarding the SNR, the performance of TSA is best among the deterministic approaches (TFA, MFA, TSA). For SNR levels of 2.48 and higher, TSAKF performs better than all other deterministic and probabilistic approaches. Regarding the object density, MFA is better than TFA, and TSA is better than MFA. Accordingly, MFAKF is better than KF, and TSAKF is better than MFAKF. TSAKF outperforms all other approaches, in particular, for difficult tracking conditions (e.g., 75 particles and more).

We have also applied all six tracking approaches to 5 real image sequences displaying dynamics of fluorescently labeled avian leukosis virus (ALV) particles. The images were acquired using a confocal microscope with a frame rate of 4 frames per minute [9]. The image dimensions vary between 512x512 pixels and 1024x1024 pixels, the number of time points ranges from 36 to 180, and the number of particles varies from 28 to 380. The image sequences differ in the

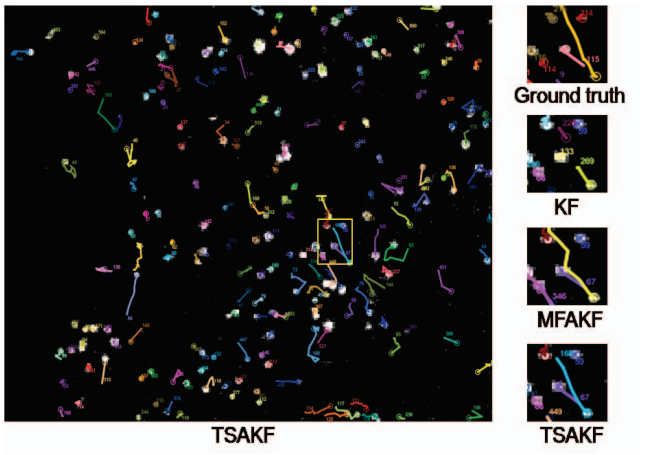


Fig. 4. A real image sequence with tracking results of TSAKF. For the selected region, tracking results of different approaches are shown.

Table 1: Tracking results of different approaches for 5 real microscopy images (mean track error $\bar{E}_{track}$ and standard deviation)

	TFA	MFA	TSA	KF	MFAKF	TSAKF
$\bar{E}_{track}$	0.345	0.321	0.243	0.298	0.284	0.218
Std.d.	0.165	0.210	0.200	0.166	0.167	0.185

level of the image noise, the object density, the motion pattern of the particles, and the number of spurious objects. Ground truth for the real images has been determined by manual tracking using the ImageJ plugin MTrackJ. A real image sequence with tracking results of TSAKF and a selected region with tracking results for different approaches are shown in Figure 4. The selected region displays real particles which exhibit different motion patterns, and cluster and uncluster. Spurious objects appear for one time point and disappear. As can be seen from Figure 4, KF generates broken trajectories because of particle clustering and MFAKF generates incorrect trajectories because of spurious objects. In comparison, TSAKF generates correct trajectories by effectively dealing with spurious objects as well as particle clustering and unclustering. The mean track error $\bar{E}_{track}$ (and standard deviation) for all 5 image sequences is shown in Table 1. It can be seen that TSA outperforms MFA which is better than TFA. Consequently, TSAKF outperforms MFAKF which is better than KF. The probabilistic approaches (KF, MFAKF, TSAKF) perform better than corresponding deterministic approaches (TFA, MFA, TSA).

4. DISCUSSION

We have presented a two-step deterministic multi-frame association finding algorithm (TSA) which is based on a temporally semi-global formulation as well as combines a spatially global and a spatially local approach. Using this multi-frame association finding algorithm we have presented a probabilistic tracking approach based on the Kalman filter. On the basis of a quantitative performance evaluation and a comparison with previous approaches we found that TSA yields the best result among the deterministic association finding algorithms by virtue of the combined optimization scheme. Consequently, the combination of TSA with the Kalman filter (TSAKF) outperforms the other probabilistic approaches (KF, MFAKF). The performance of the proposed approaches could further be improved by including a better particle detection approach which will be the subject of future work.

Acknowledgements

This work has been supported by the BMBF (FORSYS) project VIROQUANT. We also thank the graduate school HGS MathComp, University of Heidelberg.

5. REFERENCES

[1] I.F. Sbalzarini and P. Koumoutsakos, "Feature point tracking and trajectory analysis for video imaging in cell biology," *J. Struct. Biol.*, vol. 151, pp. 182–195, 2005.

[2] K. Shafique and M. Shah, "A noniterative greedy algorithm for multiframe point correspondence," *IEEE Trans. on Pattern Analysis and Machine Intelligence*, vol. 27, pp. 51–65, 2005.

[3] I. Smal, K. Draegestein, N. Galjart, W. Niessen, and E. Meijering, "Particle filtering for multiple object tracking in dynamic fluorescence microscopy images: Application to microtubule growth analysis," *IEEE Trans. on Med. Imaging*, vol. 27, pp. 789–804, 2008.

[4] W.J. Godinez, M. Lampe, S. Wörz, B. Müller, R. Eils, and K. Rohr, "Deterministic and probabilistic approaches for tracking virus particles in time-lapse fluorescence microscopy image sequences," *Med. Image Anal.*, vol. 13, pp. 325–342, 2009.

[5] N. Chenouard, I. Bloch, and J.-C. Olivo-Marin, "Multiple hypothesis tracking in microscopy images," *in Proc. ISBI'09, Boston, MA, USA*, pp. 1346–1349, July 2009.

[6] K. Jaqaman, D. Loerke, M. Mettlen, H. Kuwata, S. Grinstein, S.L. Schmid, and G. Danuser, "Robust single-particle tracking in live-cell time-lapse sequences," *Nat. Methods.*, vol. 5, pp. 695–702, 2008.

[7] L. Feng, Y. Xu, Y. Yang, and X. Zheng, "Multiple dense particle tracking in fluorescence microscopy images based on multidimensional assignment," *J. Struct. Biol.*, vol. 173, pp. 219–228, 2011.

[8] D. Sage, F.R. Neumann, F. Hediger, S.M. Gasser, and M. Unser, "Automatic tracking of individual fluorescence particles: application to the study of chromosome dynamics.," *IEEE Trans. on Image Process.*, vol. 14, pp. 1372–1383, 2005.

[9] M.J. Lehmann, N.M. Sherer, C.B. Marks, M. Pypaert, and W. Mothes, "Actin- and myosin-driven movement of viruses along filopodia precedes their entry into cells," *J. Cell Biol.*, vol. 170, pp. 317–325, 2005.